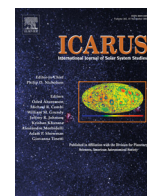




ELSEVIER

Contents lists available at ScienceDirect

Icarus

journal homepage: [www.elsevier.com/locate/icarus](http://www.elsevier.com/locate/icarus)

## Mean radius and shape of Pluto and Charon from *New Horizons* images

Francis Nimmo<sup>a,\*</sup>, Orkan Umurhan<sup>b</sup>, Carey M. Lisse<sup>c</sup>, Carver J. Bierson<sup>a</sup>, Tod R. Lauer<sup>d</sup>,  
 Marc W. Buie<sup>e</sup>, Henry B. Throop<sup>f</sup>, Josh A. Kammer<sup>e</sup>, James H. Roberts<sup>c</sup>,  
 William B. McKinnon<sup>g</sup>, Amanda M. Zangari<sup>e</sup>, Jeffrey M. Moore<sup>b</sup>, S. Alan Stern<sup>e</sup>,  
 Leslie A. Young<sup>e</sup>, Harold A. Weaver<sup>c</sup>, Cathy B. Olkin<sup>e</sup>, Kim Ennico<sup>b</sup>

<sup>a</sup> Department of Earth and Planetary Sciences, University of California Santa Cruz, Santa Cruz, CA 95064, United States

<sup>b</sup> NASA Ames Research Center, Moffett Field, CA 94035, United States

<sup>c</sup> Johns Hopkins University Applied Physics Laboratory, Laurel, MD 20723, United States

<sup>d</sup> NOAO, P.O. Box 26732, Tucson, AZ 85726, United States

<sup>e</sup> Southwest Research Institute, 1050 Walnut St. Suite 300, Boulder, CO 80302, United States

<sup>f</sup> Planetary Science Institute, 1700 E Fort Lowell Suite 106, Tucson, AZ 85719, United States

<sup>g</sup> Department of Earth and Planetary Sciences, Washington University, St. Louis, MO 63130, United States

### ARTICLE INFO

#### Article history:

Received 1 February 2016

Revised 22 June 2016

Accepted 28 June 2016

Available online xxx

#### Keywords:

Kuiper belt  
 Satellites, shapes  
 Trans-neptunian objects  
 Satellites, formation  
 Interiors  
 Thermal histories

### ABSTRACT

Approach images taken by the LORRI imaging system during the *New Horizons* spacecraft encounter have been used to determine the mean radii and shapes of Pluto and Charon. The primary observations are limb locations derived using three independent approaches. The resulting mean radii of Pluto and Charon are  $1188.3 \pm 1.6$  km and  $606.0 \pm 1.0$  km, respectively ( $2\text{-}\sigma$ ). The corresponding densities are  $1854 \pm 11$  kg/m<sup>3</sup> and  $1701 \pm 33$  kg/m<sup>3</sup> ( $2\text{-}\sigma$ ). The Charon radius value is consistent with previous Earth-based occultation estimates. The Pluto radius estimate is consistent with solar occultation measurements performed by the ALICE and Fine Sun Sensor instruments on *New Horizons*. Neither Pluto nor Charon show any evidence for tidal/rotational distortions; upper bounds on the oblateness are  $< 0.6\%$  and  $< 0.5\%$ , respectively.

© 2016 Elsevier Inc. All rights reserved.

### 1. Introduction

Knowing the mean radius of both Pluto and Charon is a prerequisite for determining their bulk density, which in turn has implications for their bulk composition and, potentially, their mode of formation. For instance, models in which Charon formed via a giant impact (Canup 2005; Desch 2015) make different predictions from models in which both bodies formed by direct collapse of gravitationally-bound clumps of “pebbles” (Nesvorný et al., 2010). Likewise, the long-wavelength shape of these bodies - departures from sphericity, such as rotational flattening - can potentially provide information on their internal structure and evolution (McKinnon and Singer, 2014). This paper provides a preliminary assessment of the mean radius and shape of both Pluto and Charon, based primarily on optical imaging provided by the *New Horizons* spacecraft during its recent flyby (Stern et al., 2015).

Prior to the *New Horizons* flyby, radii for Pluto and Charon had been estimated using Earth-based observations of stellar occultations and mutual events (Table 1). For Charon, recent

occultation results were internally quite consistent and yielded a radius of around 605 km (Person et al., 2006; Sicardy et al., 2006), with some outliers being ascribed to local topography. For Pluto, however, the existence of a thin atmosphere (e.g. Binzel and Hubbard 1997; Person et al., 2013) increased the uncertainty in radius estimates; for instance, Lellouch et al. (2009) reported a range of 1169–1193 km. Mutual event estimates were not affected by the atmosphere, but were thought to be affected by orbital uncertainties, limb darkening and albedo variations. Young and Binzel (1994) derived radii for Pluto and Charon of  $1179 \pm 24$  km and  $629 \pm 21$  km, respectively. Buie et al. (1992) reported values for Pluto and Charon of  $1150 \pm 7$  km and  $593 \pm 10$  km, respectively; by using other techniques (stellar occultations and Hubble images, respectively) to fix the radius and orbit of Charon, the radius of Pluto was later updated to 1189.5 km by Tholen (2014).

Because of these uncertainties the densities of Pluto and Charon were barely distinguishable at the  $2\text{-}\sigma$  level (e.g. Brozovic et al., 2015). As initially reported in Stern et al. (2015) and elucidated in more detail here, one of the major results of the *New Horizons* mission is that Pluto is definitely denser than Charon, by about 9%.

Pluto and Charon today occupy a doubly-synchronous state (Dobrovolskis et al., 1997; Buie et al., 1997). If they respond

\* Corresponding author.

E-mail address: [fnimmo@es.ucsc.edu](mailto:fnimmo@es.ucsc.edu) (F. Nimmo).

**Table 1**

Previous estimates of Pluto and Charon radii, modified from McKinnon et al. (1997).

Reference	Pluto radius (km)	Charon radius (km)	Notes
Dunbar and Tedesco (1986)	1150 ± 50	750 ± 50	
Reinsch and Pakull (1987)	1100 ± 70	580 ± 50	
Tholen and Buie (1988)	1142 ± 9	596 ± 17	
Eshleman (1989)	1180 ± 23	–	
Tholen and Buie (1990)	1151 ± 6	593 ± 13	
Elliot and Young (1991)	–	>601.5	
Elliot and Young (1992)	1206 ± 11	–	Positive thermal gradient
Young (1992)	1191 ± 20	642 ± 11	
Buie et al. (1992)	1150 ± 7	593 ± 10	
Millis et al. (1993)	1195 ± 5	–	Positive thermal gradient
Reinsch et al. (1994)	1152 ± 7	595 ± 5	Recalibrated semi-major axis
Young and Binzel (1994)	1179.5 ± 23.5	629 ± 21	Recalibrated semi-major axis
Albrecht et al. (1994)	1160 ± 12	635 ± 13	
Buratti et al. (1995)	1155 ± 20	612 ± 30	
Person et al. (2006)	–	606.0 ± 1.5	
Sicardy et al. (2006)	–	603.6 ± 1.4	
Lellouch et al. (2009)	1169–1193	–	
Stern et al. (2015)	1187 ± 4	606 ± 3	<i>New Horizons</i>
This work	1188.3 ± 1.6	606.0 ± 1.0	<i>New Horizons</i>

to the present-day tidal and rotational potentials as fluid bodies, then Pluto will closely approximate an oblate spheroid, while Charon will be triaxial. For Pluto, the flattening is approximated by  $R\omega^2 h_2/2g$  (e.g. Murray and Dermott, 2000; also see Section 5 below). Here  $R$  is the radius,  $\omega$  the rotation angular frequency,  $h_2$  a dimensionless constant of order unity for a fluid, and  $g$  the surface gravity. Deviations from sphericity for a present-day, fluid Pluto are thus expected to be  $\sim 0.05\%$ , with similar deviations expected at Charon. In principle, these deviations can be used to determine a body's moment of inertia (as long as it is behaving in a fluid-like fashion); such techniques have been used with some success for the moons of Jupiter and Saturn (e.g. Dermott and Thomas, 1988; Oberst and Schuster, 2004; Thomas et al., 1998, 2007).

However, earlier in their history, Pluto and Charon were likely closer together and their spin rates were correspondingly faster (Dobrovolskis et al., 1997). Thus, in principle Pluto and/or Charon could have “frozen in” rotational and/or tidal bulges at an early epoch in their history and maintained such “fossil” bulges to the present day. That is, they could resemble the Earth's Moon (e.g. Garrick-Bethell et al., 2014) or Iapetus (Castillo-Rogez et al., 2007), both of which possess large fossil bulges inconsistent with their present-day spin rates. Whether or not a body can maintain a fossil bulge depends largely on its thermal evolution: bodies that are warm and deformable, or have weak lithospheres or a subsurface ocean, will not maintain such a bulge, while cold and rigid bodies can. Thus, the presence or absence of a fossil bulge at Pluto or Charon provides a constraint on these bodies' internal structure and thermal and orbital evolution (Robuchon and Nimmo, 2011; McKinnon and Singer, 2014).

The remainder of this paper is organized as follows. We focus primarily on results derived from images taken by *New Horizons*, though we do make limited use of constraints from other techniques. Section 2 describes the primary observation set used to determine radius and shape, while Section 3 describes the techniques used to convert a single image into an estimate of radius and shape. This section includes a preliminary analysis of likely uncertainties by analyzing synthetic data sets. Section 4 extends the approach outlined in Section 3 to fitting results from multiple

images simultaneously, while Section 5 summarizes our results and discusses the implications. The Appendices provide further details of specific aspects of our analysis.

## 2. Observations

### 2.1. LORRI

The primary instrument used in this analysis was the Long-Range Reconnaissance Imager (LORRI), the characteristics of which are described in Cheng et al. (2008). In brief, LORRI comprises a  $1024 \times 1024$  pixel CCD positioned at the Cassegrain focus of a 20.8 cm Ritchey–Chrétien telescope. Images are obtained in white-light over a 350–850 nm bandpass. The mechanical design of the camera ensures high-stability of the optics within the spacecraft environment. Significantly, the camera is operated without a mechanical shutter. Some charge does accumulate during the short frame-transfer time at readout, which is subtracted as part of standard image reduction.

A key parameter in the following analysis is the angular width of a LORRI pixel, because this is required to convert spacecraft range to a length-scale at the image. Based on images of NGC 3532 taken in 2013, the value adopted in this work is  $4.963571 \pm 0.000038 \mu\text{rad}/\text{pixel}$ , an update from the value previously reported in Cheng et al. (2008). The small distortions introduced by the LORRI optics have been quantified (Owen and O'Connell, 2011) and their effect is discussed in more detail below and in Appendix E. The point-spread function (PSF) of LORRI is not axisymmetric (Noble et al., 2009), but analysis of synthetic images including a realistic PSF suggests that shape determination is negligibly affected by this particular effect (Appendix A).

During the approach phase, LORRI took a series of images of Pluto and Charon at increasingly higher resolution. Our analysis was based on all approach images downlinked as of August 2015. In this work we have only used single-frame images, because fitting a substantial fraction of the illuminated limb is required in order to establish the center of figure and to search for any oblateness. Mosaics of Pluto and Charon at higher resolutions do exist, but were not used in this study. High-phase departure (“lookback”) images of Pluto reveal a pronounced atmospheric haze (Stern et al., 2015) which makes identification of the solid surface challenging; those images were not used in the current analysis.

Table 2 presents details of the images used. The highest resolution images are at about 3.7 km/pixel and 2.3 km/pixel for Pluto and Charon, respectively. Among the images used there is a range in resolution of about a factor of 3 (for Pluto) and about 4 (for Charon); adding earlier images would increase the range of longitudes covered, but at the expense of even poorer resolution. The tabulated geometric parameters, discussed in more detail below, are based on the *15sci\_rhr* (od122) reconstructed kernel (Steffl et al., 2016) and were derived by the Navigation team using optical navigation and radiometric data following the encounter (see e.g. Jackman et al., 2016; Pelletier et al., 2016). For convenience (and because some images actually combine multiple exposures, see below) we refer to images as “visitXX” with a subscript denoting Pluto or Charon. LORRI images are uniquely identified by their clock time (MET); thus, visit73p can also be referred to as LOR\_0299124574 (see Tables 2 and 3).

### 2.2. Combining multiple images

Except near closest approach, the sequencing resulted in two or more images being taken at almost identical epochs. The small, random drift in spacecraft pointing between exposures effectively “dithers” the images in a sequence. This dithering can be used to combine the individual images to produce a single summed and

Download English Version:

<https://daneshyari.com/en/article/5487351>

Download Persian Version:

<https://daneshyari.com/article/5487351>

[Daneshyari.com](https://daneshyari.com)